

Electronic supporting Information

Albumin-targeting of an oxaliplatin-releasing platinum(IV) prodrug results in pronounced anticancer activity due to endocytotic drug uptake *in vivo*

Hemma Schueffl^{a§}, Sarah Theiner^{b§}, Gerrit Hermann^b, Josef Mayr^c, Philipp Fronik^c, Diana Groza^a, Sushilla van Schonhooven^a, Luis Galvez^b, Nadine Sommerfeld^c, Arno Schintlmeister^d, Siegfried Reipert^e, Michael Wagner^d, Robert M. Mader^f, Gunda Koellensperger^b, Bernhard K. Keppler^{c,§}, Walter Berger^{a,f}, Christian R. Kowol^{c,f*}, Anton Legin^{c*}, Petra Heffeter^{a,f*}

^a Institute of Cancer Research, and Comprehensive Cancer Center, Medical University of Vienna, Borschkegasse 8a, A-1090 Vienna, Austria

^b Institute of Analytical Chemistry, Faculty of Chemistry, University of Vienna, Waehringer Str. 38, A-1090 Vienna, Austria

^c Institute of Inorganic Chemistry, Faculty of Chemistry, University of Vienna, Waehringer Str. 42, A-1090 Vienna, Austria

^d Centre for Microbiology and Environmental Systems Science, Division of Microbial Ecology and Large-Instrument Facility for Environmental and Isotope Mass Spectrometry, University of Vienna, Djerassiplatz 1, A-1030 Vienna, Austria

^e Core Facility Cell Imaging and Ultrastructure Research, University of Vienna, University Biology Building (UBB), Djerassiplatz 1, A-1030 Vienna, Austria

^f Department of Medicine I and Comprehensive Cancer Center, Medical University of Vienna, Waehringer Guertel 18-20, 1090 Vienna, Austria

[§] Research Cluster "Translational Cancer Therapy Research", University of Vienna and Medical University of Vienna, Vienna, Austria

§ These authors contributed equally to the main findings of this manuscript

Table of Contents

1. Experimental part.....	4
Drugs and chemicals.....	4
Cell culture	4
Cellular albumin uptake determined by flow cytometry.....	4
Cellular albumin uptake determined by fluorescence microscopy	4
Cytotoxicity assays	5
Cellular platinum uptake determined by inductively coupled plasma-mass spectrometry (ICP-MS) measurement	5
Colony formation assay	5
Western blot analysis	6
Animals.....	6
Tumor distribution of FITC-labeled maleimide.....	6
Immune fluorescence staining of endomucin on cryo-sections.....	7
Allograft anticancer activity experiments	7
Pharmacokinetic of single dose in serum.....	8
SEC- and flow injection-ICP-MS measurements of serum samples.....	8
Organ and tumor distribution experiments	9
Determination of total platinum concentration in mice tissues by ICP-MS	10
Multi-element analysis in tumor sections by LA-ICP-TOFMS	10
Synthesis of the isotopically-labeled complex KP2603.....	11
TEM analysis and sample preparation.....	13
NanoSIMS analysis, image processing and numerical data evaluation	14
NanoSIMS image processing and numerical data evaluation	14
Statistics	16
2. Supplementary Figures.....	17
3. Supplementary Tables	34
4. References.....	35

1. Experimental part

Drugs and chemicals

KP2156, KP2157 and oxaliplatin were prepared as described previously.¹ All other substances were purchased from Sigma-Aldrich (St. Louis, USA). All solutions were freshly prepared before usage.

Cell culture

For *in vitro* experiments, the murine (Balb/c) colon cancer cell model CT26 (purchased from American Type Culture Collection, Manassas, VA, USA) was used. Cells were grown in DMEM/F12 supplemented with 10% fetal calf serum (FCS). All cell culture media and reagents were purchased from Sigma-Aldrich Austria.

Cellular albumin uptake determined by flow cytometry

CT26 cells were plated in 6-well plates (3×10^5 cells in 1 mL per well) and left to recover for 24 h. FITC-conjugated bovine serum albumin (10 μ M, A9771, Sigma Aldrich) was diluted with serum-free RPMI medium and added to the cells. After 1 and 3 h the cells were harvested by trypsinization, diluted in phosphate-buffered saline (PBS) and the fluorescence was measured by flow cytometry at 530 nm using a BD Fortessa flow cytometer.

Cellular albumin uptake determined by fluorescence microscopy

Cells were seeded (1.2×10^4 cells/well) in 8-well chamber slides (Falcon™, Corning Brand, USA) and were incubated in growth medium with 10% FCS for 48 h to allow proper cell adhesion. To determine the cellular uptake of albumin at different time points, the cells were treated with 10 μ M FITC-labeled albumin (dissolved in serum-free RPMI medium) for 1 and 3 h. After the incubation time, the medium was removed from the chambers. Next, the cells were fixed with 4% paraformaldehyde (PFA) in PBS for 15 min, followed by four washing steps with PBS. Additionally, 4',6-diamidino-2-phenylindole (DAPI) and wheat germ agglutinin (WGA) staining was performed by incubating the slide with staining solution containing 0.3% DAPI and 0.45% rhodamine-labeled WGA (Vector Laboratories, Germany). Next, the slide was mounted with non-hardening mounting medium (Vectashield® Mounting Media, Vector, USA), followed by fluorescence measurement with confocal microscope (Zeiss, Germany) and image processing via ZEN lite software (Zeiss, Germany).

Cytotoxicity assays

Cells were plated in 96-well plates (1.2×10^4 cells in 100 μ L per well) and left to recover for 24 h. Subsequently, the cells were incubated for 5 h in rising concentrations of the endocytosis inhibitors methyl-beta-cyclodextrin (M β CD, caveolin-dependent endocytosis), chlorpromazine (CHP, clathrin-dependent endocytosis) and 5-(*N*-ethyl-*N*-isopropyl)amiloride (EIPA, macropinocytosis). All substances were freshly dissolved either in water (M β CD and CHP) or dimethyl sulfoxide (DMSO) (EIPA) before further dilution in cell culture medium. DMSO concentrations were always below 1%. After 24 h incubation, cell viability was analyzed using an MTT-based assay (EZ4U, Biomedica, Austria) following the manufacturer's recommendations.

Cellular platinum uptake determined by inductively coupled plasma-mass spectrometry

(ICP-MS) measurement

CT26 cells were plated in 6-well plates (9×10^5 cells in 1 mL per well) and left to recover for 24 h. Drugs were pre-incubated as described in the colony formation assay below and then added to the cells, in the indicated concentrations, in duplicates. Drug solution was also added to blank wells without cells in triplicates, in order to assess absorption of the compounds to the plastic of the well. The protocol by Egger et al.² was followed for sample processing, measurement and data evaluation. The platinum concentration was determined by ICP-MS analysis. Platinum and rhenium standards were derived from CPI International (Amsterdam, The Netherlands). The total platinum content was determined with a quadrupole-based ICP-MS instrument Agilent 7500ce (Agilent Technologies, Waldbronn, Germany) equipped with a MicroMist nebulizer at a sample uptake rate of approximately 0.25 mL min⁻¹. Argon was used as plasma gas (15 L min⁻¹) and as carrier gas (~ 1.1 L min⁻¹). The dwell time was set to 0.3 s and the measurements were performed in 10 replicates. Rhenium served as internal standard for platinum. The Agilent MassHunter software package (Workstation Software, version B.01.01, 2012) was used for data processing.

Colony formation assay

CT26 cells were plated in 24-well plates (250 cells in 500 μ L growth medium per well) and left to recover for 24 h in the incubator. Before adding to test compounds to the cells, they were preincubated for 2 h at 37°C with FCS (10% of the volume of the drug solution in the end) followed by further dilution to the working stocks using serum-free RPMI medium. After 8-14 days, the cells were fixed with methanol for 20 min at 4°C and stained with crystal violet

(0.01% in PBS). The fluorescence of crystal violet was detected by the Typhoon scanner (Typhoon TRIO Variable Mode Imager, GE Healthcare Life Sciences) after excitation by the red laser (633 nm). Quantification was done by ImageJ software. The received data was visualized as dose-response curves by Graph Pad Prism 5 software (Graph Pad software, USA).

Western blot analysis

To trace back the enhanced activity of the platinum(IV) drugs in combination with the reducing agent ascorbic acid (AA) to the induction of double-strand breaks, the DNA damage marker pH2A.X was determined by Western blot analysis. First, CT26 cells were seeded in a 6-well plate (5×10^5 cells/mL/well) and after 24 h recovery, treated with the drug in different concentrations with or without 100 μ M AA for 5 h. Next, cells were harvested, proteins were isolated resolved by SDS/PAGE, and transferred onto a polyvinylidene difluoride membrane for Western blotting as described previously.³ The following antibodies were used: pH2A.X (#2577, Cell Signaling Technology, USA), and β -actin (A5441, Sigma Aldrich). All primary antibodies were used in 1:1000 dilutions in 3% BSA-and 0.1%-Tween-20-containing Tris-buffered saline. Additionally, horseradish peroxidase-labeled secondary antibodies anti-mouse (#7076 Cell Signaling Technology, USA) and anti-rabbit (A0168, Sigma-Aldrich) were used at working dilutions of 1:10000.

Animals

Eight- to twelve-week-old Balb/c mice were purchased from Envigo Laboratories (San Pietro al Natisone, Italy). The animals were kept in a pathogen-free conditions, controlled environment with 12 h light–dark cycle and every procedure was done in a laminar airflow cabinet. All experiments were approved by the Ethics Committee for the Care and Use of Laboratory Animals at the Medical University Vienna (proposal number BMWF-66.009/0084-II/3b/2013) and performed according to the guidelines from the Austrian Animal Science Association and from the Federation of European Laboratory Animal Science Associations (FELASA).

Tumor distribution of fluorescein-labeled maleimide

Female Balb/c mice were injected s.c. with 50 μ L cell suspension containing 5×10^5 CT26 cells in growth medium without serum. Once the tumors reached 10 mm length, the animals were treated with fluorescein-labeled maleimide (16 mg kg^{-1} dissolved in 0.9% NaCl solution including 1% DMSO and 10% propylene glycol) i.v. (2 mice per substance and time point). After 30 min or 5 h, the mice were sacrificed by cervical dislocation and tumor samples were

harvested. Subsequently, the tissues were sliced, embedded in O.C.T™ medium (Tissue-Tek®, Sakura® Finetek, USA), frozen on dried ice and stored at -80°C.

Immune fluorescence staining of endomucin on cryo-sections

The O.C.T. blocks containing the tissue pieces were sliced to 5 µm sections at -20°C using a cryomicrotome (Cryostar NX70, ThermoScientific, USA). First, the cryo slides were defrosted and the tissue was fixed with 4% PFA in PBS. Afterwards, the slides were blocked with blocking buffer (PBS containing 1% BSA, 5% goat serum and 0.1% Triton 100-X) for 1 h. Then, the tissues were incubated with the primary endomucin monoclonal antibody (eBioV.7C7 (V.7C7), eBioscience™, ThermoFisher, USA) diluted 1:800 in blocking buffer for 1.5 h at RT. Subsequently, the samples were incubated with secondary anti rat antibody solution (diluted 1:400 in PBS containing 5% goat serum) labeled with TRITC (Jackson ImmunoResearch, USA) for 1 h at RT. Then, the tissues were mounted in non-hardening mounting medium with DAPI (Vectashield® Mounting Media, Vector, USA). Finally, the fluorescence of the samples was measured on a fluorescence microscope (eclipse 80i, Nikon, Japan), where also pictures were taken with a mono-color camera (QR2 Nikon, Japan) and further processed with the imaging software Nis-elements-Br version 4.3 (Nikon, Japan).

Allograft anticancer activity experiments

CT26 cells (5×10^5 in serum-free medium) were injected subcutaneously into the right flank of male Balb/c mice. Therapy was started when tumor nodules were palpable (day 4). Animals were treated with KP2156 (18 mg kg^{-1} i.v. dissolved in 0.9% NaCl), KP2157 (18 mg kg^{-1} i.v. dissolved in 0.9% NaCl) and the equimolar dose of oxaliplatin (9 mg kg^{-1} i.v. dissolved in 5% glucose) on day 4, 7, 11 and 14 after cell injection. Animals were controlled for distress development every day and tumor size was assessed regularly by caliper measurement. Tumor volume was calculated using the formula: $(\text{length} \times \text{width}^2)/2$. In the overall survival experiments, mice were sacrificed by cervical dislocation in the case of a tumor length > 20 mm or tumor ulceration. For histological and ICP-MS evaluations, 4 animals per treatment group were sacrificed by cervical dislocation on day 15 and tumors collected. The samples divided into several pieces and either fixed and paraffin-embedded or nitrogen-frozen and stored at -20°C for further analysis.

Histological evaluations

Tumors were fixed in 4% formaldehyde for 24 h (Carl Roth, # P087.3) and paraffin-embedded using a KOS machine (Milestone). For histological evaluation, tumor tissues were sliced in

3 μm thick sections. The immunohistochemistry was performed as described previously.⁴ Briefly, for evaluation of the albumin content in untreated CT26 tumors, the tissue was deparaffinized and rehydrated. Subsequently, the samples were heated for 10 min in 10 mM citrate buffer (pH 6.0) followed by incubation with the albumin primary antibody (PA5-85166, Thermo Fisher: dilution 1:2000 at RT for 1 h) diluted in antibody diluent (#8112, Cell Signaling Technology, USA). Binding of primary antibodies was detected with the UltraVision LP detection system according to the manufacturer's instructions (Thermo Fisher Scientific), followed by incubation with 3,3'-diaminobenzidine (Dako, cat.no. K3468) and counterstaining with hematoxylin Gill III (Merck, cat.no. 1.05174.0500).

As a first step for tissue evaluation of the allograft anticancer activity experiments, a hematoxylin and eosin stain was performed. Next, apoptotic and mitotic cells were counted in blinded samples (40x magnification). Additionally, immunohistochemical evaluations of cl. caspase-3 (#9664, Cell Signaling Technology, USA: at 4°C overnight, dilution 1:1000) and Ki-67 (#12202, Cell Signaling Technology, USA: at RT for 30 min, dilution 1:200) were performed to detect apoptotic as well as proliferating cells, respectively. Therefore, the same work flow as for the albumin staining described above was used. Additionally, the slides were scanned (40x objective, Panoramic Midi scanner, 3DHistech, Hungary) and further evaluated by Definiens software.

Pharmacokinetic of single dose in serum

Male Balb/c mice (n=4 per treatment) were treated with KP2156 (18 mg kg⁻¹ i.v. dissolved in 0.9% NaCl), KP2157 (18 mg kg⁻¹ i.v. dissolved in 0.9% NaCl) or the equimolar dose of oxaliplatin (9 mg kg⁻¹ i.v. dissolved in 5% glucose). After 5 min or 20 min, 5 h, 24 h, 72 h, 1 week and 2 weeks blood was collected via the facial vein. Serum was isolated of the collected blood samples by centrifugation at 900 g for 10 min for two times and stored at -20 °C. Platinum content was detected by SEC-ICP-MS and flow injection (FI)-ICP-MS measurements.

SEC- and flow injection-ICP-MS measurements of serum samples

The analysis via size exclusion chromatography (SEC)-ICPMS was carried out as described before¹ on a Perkin Elmer Series 200 HPLC system coupled to a Perkin Elmer Elan DRC II ICP-QMS system. For separation by SEC, the column Waters Biosuite 125 4 μm UHR SEC, 4.6 x 300 mm was used. The following chromatographic conditions were used: injection volume: 10 μL (partial loop injection 20 μL), flow rate: 0.30 mL min⁻¹; isocratic elution; CH₃COONH₄ (100 mM, pH = 6.8) was employed as mobile phase. The following masses were recorded with ICP-MS:

$^{32}\text{S}^{16}\text{O}^+$ and $^{195}\text{Pt}^+$. To determine reference elution times for important sulphur-containing proteins found in blood serum - like albumin or glutathione – a size ladder was first measured (Table S1). Albumin dimers are eluted after 8.5 minutes, while albumin monomers have an elution time of 9.5 min.

Table S1: Resulting size ladder measured by SEC-ICP-MS.

Compound	Time (min)	Size (kDa)
Albumin dimer	8.5	132
Albumin	9.5	66
Superoxide dismutase	11.1	37
Glutathione disulfide	13.2	0.6

Quantification of platinum in serum samples was performed by flow injection-ICP-MS analysis. Measurements were performed using an Agilent 1260 Infinity Bio-inert HPLC system (Agilent Technologies, Waldbronn, Germany) hyphenated to an Agilent 8800 ICP-MS/MS instrument (Agilent Technologies, Tokyo, Japan). The following chromatographic conditions were used: injection volume: 5 μL ; flow rate: 0.30 mL min^{-1} ; isocratic elution; $\text{CH}_3\text{COONH}_4$ (50 mM, pH 6.8) was employed as mobile phase. Platinum was monitored in no gas mode with an integration time of 0.1 s.

Organ and tumor distribution experiments

CT26 cells (5×10^5 in serum-free medium) were injected into the right flank of male Balb/c mice. Once the tumors reached 10 mm length, the animals were treated with KP2156 (18 mg kg^{-1} i.v. dissolved in 0.9% NaCl), KP2157 (18 mg kg^{-1} i.v. dissolved in 0.9% NaCl) or the equimolar dose of oxaliplatin (9 mg kg^{-1} i.v. dissolved in 5% glucose). After 5 h, 24 h, 48 h, 168 h and 336 h, the animals (4 per time point and treatment group) were anesthetized and urine was collected via bladder puncture (if available). Additionally, tumors, liver and kidney tissues were harvested, stored at -20°C and further processed platinum measurements via ICP-MS. For LA-ICP-MS, one half of the 5 h KP2156 and oxaliplatin treated tumors were embedded in O.C.TTM medium, frozen on dried ice and stored at -80°C .

Determination of total platinum concentration in mice tissues by ICP-MS

Digestion of mice tissue samples (tumor, kidney, liver, serum, blood pellet etc.) was performed as described previously⁵ using a microwave system Discover SP-D (CEM Microwave Technology, Germany) with nitric acid ($\geq 69\%$, p.a., TraceSelect, Fluka). Digested samples were diluted in Milli-Q water (18.2 M Ω cm, Milli-Q Advantage, Darmstadt, Germany). The platinum concentration was determined by ICP-MS analysis using the same instrumental conditions as for platinum analysis in cells.

Multi-element analysis in tumor sections by LA-ICP-TOFMS

An Analyte Excite Excimer 193nm laser ablation system (Teledyne Photon Machines, Bozeman, MT, USA) was coupled to an *icp*TOF 2R (TOFWERK AG, Thun, Switzerland) TOF-based ICP-MS instrument. The laser ablation system was equipped with the HeExII volume ablation cell and the aerosol rapid introduction system (ARIS). Through the low-dispersion mixing bulb of the ARIS, an Ar make-up gas flow (~ 1 L min⁻¹) was introduced into a He carrier gas flow (0.50 L min⁻¹) before entering the plasma. The LA and ICP-TOFMS settings were optimized on a daily basis while ablating NIST SRM612 glass certified reference material (National Institute for Standards and Technology, Gaithersburg, MD, USA). Laser ablation sampling was performed in fixed dosage mode 1, at a repetition rate of 20 Hz and using a circular spot size of 20 μ m in diameter. Tumor sections were removed quantitatively using a fluence of 1.0-1.5 J cm⁻².

The *icp*TOF 2R ICP-TOFMS instrument has a specified mass resolution ($R = m/\Delta m$) of 6000 (full width half-maximum definition), which allows the analysis of ions from $m/z = 14$ -256. The integration and read-out rate match the laser ablation repetition rate. The instrument was equipped with a torch injector of 2.5 mm inner diameter and nickel sample and skimmer cones with a skimmer cone insert of 2.8 mm in diameter. A radio frequency power of 1440 W, an auxiliary Ar gas flow rate of ~ 0.80 L min⁻¹ and a plasma Ar gas flow rate of 15 L min⁻¹ was used.

Data was recorded using TofPilot 1.3.4.0 (TOFWERK AG, Thun, Switzerland). Post-acquisition data processing was performed with Tofware v3.2.0, which is a TOFWERK data analysis package and used as an add-on on IgorPro (Wavemetric Inc., Oregon, USA). The data was further processed with HDIP version 1.3.1.1038 (Teledyne Photon Machines, Bozeman, MT, USA).

Synthesis of the isotopically-labeled complex KP2603

(SP-4-3)-D10-cyclohexane-1,2-diaminedichloridoplatinum(II) was synthesized from D10-cyclohexene according to literature.⁶ β -Alanine- $^{13}\text{C}_3,^{15}\text{N}$ and maleic anhydride- $^{13}\text{C}_4$ were purchased from Sigma-Aldrich (St. Louis, USA). All other reagents and solvents were obtained from commercial suppliers and used without further purification. Elemental analyses were performed by the Microanalytical Laboratory of the University of Vienna on a Perkin Elmer 2400 CHN Elemental Analyzer. Electrospray ionization (ESI) mass spectra were recorded on a Bruker amaZon SL ion trap mass spectrometer. High resolution mass spectra were measured on a Bruker maXis™ UHR ESI time of flight instrument. Expected and experimental isotope distributions were compared. ^1H and ^{13}C NMR one- as well as two-dimensional spectra were recorded in CDCl_3 , $\text{DMSO}-d_6$, or $\text{DMF}-d_7$ with a Bruker FT-NMR AV NEO 500 MHz spectrometer at 500.10 (^1H) and 125.75 (^{13}C) MHz at 298 K. Chemical shifts (ppm) were referenced internal to the solvent residual peaks.

Synthesis of 3-(2,5-dioxo-2,5-dihydro-1H-pyrrol-1-yl-2,3,4,5- $^{13}\text{C}_4$ -1- ^{15}N)propanoic-1,2,3- $^{13}\text{C}_3$ acid.

100 mg of β -Alanine- $^{13}\text{C}_3,^{15}\text{N}$ (1.07 mmol) and 110 mg of maleic anhydride- $^{13}\text{C}_4$ (1 eq., 1.07 mmol) were suspended in 2 mL of acetic acid and heated to reflux for 2 h at 170 °C. The solvent was removed under reduced pressure and the crude product was purified via preparative HPLC on a Waters XBridge C18 column using H_2O (+0.1% HCOOH) and 6% acetonitrile (+0.1% HCOOH) isocratically. The collected product fractions were lyophilized and dried under reduced pressure to yield a white powder. Yield: 72 mg (38%). HRMS in ACN + 1% H_2O (negative): calcd. for [$^{13}\text{C}_7\text{H}_7^{15}\text{NO}_4 - \text{H}$]⁻: 176.0497, found: 176.0503. ^1H NMR (500.1 MHz, CDCl_3): δ = 7.04–6.43 (m, 2H, $J_{1\text{H}-^{13}\text{C}} = 187$ Hz, CH), 3.83–3.66 (m, 2H, $J_{1\text{H}-^{13}\text{C}} = 140$ Hz, CH_2), 2.94–2.55 (m, 2H, $J_{1\text{H}-^{13}\text{C}} = 130$ Hz, CH_2) ppm.

Synthesis of 1-(2-(isocyanato- ^{13}C)ethyl-1,2- $^{13}\text{C}_2$)-1H-pyrrole-2,5-dione-2,3,4,5- $^{13}\text{C}_4$ -1- ^{15}N .

70.2 mg of the maleimidopropionic acid (396.4 μmol) were dissolved in 5 mL of acetone. The solution was cooled to –5 °C and 60.5 μL of triethylamine (1.1 eq., 436 μmol) were added dropwise. Thereafter, 41.5 μL ethyl chloroformate (1.1 eq., 436 μmol) in 1 mL of acetone were added dropwise. The solution was stirred for 10 min and 25.8 mg sodium azide was added. The cooling bath was removed and stirring was continued for another 30 min. Then, the

reaction mixture was poured into 80 mL of H₂O and the reaction intermediate extracted with toluene (5 x 20 mL). The collected organic phases were dried over MgSO₄ and filtrated. Thereafter, the organic solution was heated to reflux at 140 °C for 90 min. Finally, the solvent was removed and dried under reduced pressure to yield a yellow liquid which was directly used for coupling to platinum(IV) without further analysis. Yield: 35 mg (51%).

*Synthesis of (OC-6-33)-[(1R,2R)-cyclohexane-d₁₀-1,2-diamine]
dihydrodioxalatoplatinum(IV)*

50 mg of D₁₀-labeled oxaliplatin were suspended in 1 mL of triple distilled H₂O. After the addition of 1 mL of H₂O₂ (30%), the suspension was stirred for 20 h in the dark. Thereafter, the solvent was removed under reduced pressure, the residue was taken up in MeOH and the product was fully precipitated by addition of Et₂O. The precipitate was centrifuged, the solvent decanted, the product again washed with Et₂O and, after centrifugation and decantation of the Et₂O, dried under reduced pressure to yield a white powder. Yield: 52 mg (96%). MS in MeOH (positiv): calcd. for [C₈H₆D₁₀N₂O₆Pt + Na]⁺: 464.23, found: 464.31. ¹H NMR (500.1 MHz, DMSO-d₆): δ = 7.69–7.54 (m, 2H, NH₂), 6.84–6.69 (m, 2H, NH₂) ppm.

*Synthesis of (OC-6-13)-[(1R,2R)-cyclohexane-d₁₀-1,2-diamine][bis(2-(2,5-dioxo-2,5-dihydro-1H-pyrrol-1-yl-2,3,4,5-¹³C₄-1-¹⁵N)ethyl-1,2-¹³C₂)carbamoxyloxy-¹³C)oxalatoplatinum(IV)
(KP2603).*

35 mg of the maleimido isocyanate (2.45 eq., 197 μmol) and 36 mg of the dihydrodioxaliplatin (82 μmol) were transferred into a Schlenk tube and set under argon atmosphere. After the addition of 1 mL of dry DMF, the suspension was stirred for 16 h. The solvent of the resulting clear solution was removed under reduced pressure, the residue was taken up in MeOH and the crude product was precipitated by addition of Et₂O. The precipitate was centrifuged, the solvent decanted, the crude product again washed with Et₂O and, after centrifugation and decantation of the Et₂O, dried under reduced pressure. Thereafter, the crude product was dissolved in H₂O (+0.1% HCOOH) and purified by preparative HPLC on a Waters XBridge C18 column with 86:14 H₂O (+0.1% HCOOH):ACN (+0.1% HCOOH) isocratically. The collected product fractions were lyophilized and dried under reduced pressure to yield a white powder. Yield: 31 mg (48%). Elemental analysis: calcd. for C₈¹³C₁₄H₁₈D₁₀N₄¹⁵N₂O₁₂Pt (%): C, 33.47; H, 3.56; N, 10.64. Found (%): C, 33.28; H, 3.67; N, 10.32. HRMS in ACN + 1% H₂O

(positive): calcd. for $[M + Na]^+$: 812.2582, found: 812.2336. 1H NMR (500.1 MHz, DMF- d_7): δ = 10.00–9.74 (m, 2H, NH_2), 8.79 – 8.45 (m, 2H, NH_2), 7.32 – 6.72 (m, 6H, CH and NH), 3.81–3.44 (m, 2H, CH_2 , partially below H_2O), 3.67–3.29 (m, 4H, CH_2 , partially below H_2O), 3.43–3.05 (m, 2H), 3.18–2.92 (m, 2H, CH_2 , partially below the DMF- d_7 signal) ppm. ^{13}C NMR (125.75 MHz, DMF- d_7): δ = 172.1–170.4 (m, NC=O), 165.1 (s, OC=O), 135.4–133.8 (m, CH), 39.4 (d, J = 28 Hz, $NHCH_2$), 37.6 (dd, J = 38 and 10 Hz, CH_2N) ppm. Due to the very high intensities of the ^{13}C -labeled atoms the non-labeled signals could not be observed. $^{195}Pt[^1H]$ NMR (107.38 MHz, DMF- d_7): δ = 3210 ppm.

TEM analysis and sample preparation

For the TEM and NanoSIMS analysis, CT26-bearing mice were treated with KP2603 four-times for two weeks as described in the allograft model paragraph. Tumor tissue samples were collected 24 h after the last treatment, cut into 1-2 mm³ pieces and immediately pre-fixed in 2.5% glutaraldehyde in 0.1 M sodium cacodylate buffer (0.75 mL, pH 7.3, 2 h, RT). After pre-fixation the tissue blocks were cut smaller (<1 mm³) and transferred into fresh fixative solution (0.5 mL, 2.5% glutaraldehyde in 0.1 M cacodylate buffer) at RT for 4 h. After fixation the samples were washed with cacodylate buffer (3 \times , 10 min), and postfixed with 1% OsO₄ (dissolved in 0.1 M sodium cacodylate buffer overnight) for 2 h. After washing with cacodylate buffer (2 \times , 10 min) the samples were dehydrated in an ascending ethanol series (30%, 50%, 2 \times 70%, 90% and 2 \times dried 100% ethanol, 10 min each). 100% ethanol was then replaced with pure propylene oxide (2 \times for 5 min, 1 \times for 10 min). The samples were infiltrated and embedded in low viscosity resin (LVR, Agar Scientific). The samples in pure LVR were incubated at 130 mbar vacuum for 1 h prior to polymerization. The resin blocks were polymerized in the oven at 65 °C for 96 h. Two consecutive thin sections (100 nm in thickness) were cut with a diamond knife (Diatome) by using an ultramicrotome (Ultracut S; Leica Microsystems). Both sections were placed on Formvar/carbon- coated slot- or finder grids made of copper (Agar Scientific) to allow consecutive TEM and 2 \times NanoSIMS measurements (platinum and isotopic label measurements). For electron microscopy the sections were counterstained with uranyl acetate and lead citrate and imaged in a TEM Libra 120 (Zeiss) at 120 kV. Images were acquired by using a bottom stage digital camera, Olympus Sharp: eye TRS (4 MP), and iTEM software (Soft Imaging System GmbH). The areas chosen for SIMS analysis were investigated with TEM prior to elemental imaging.

NanoSIMS analysis, image processing and numerical data evaluation

NanoSIMS analysis was carried out on a NS 50L Cameca instrument (Gennevilliers, France) as described previously.⁷ Briefly, the detectors of the multicollecion assembly were positioned to enable parallel detection of $^{16}\text{O}^1\text{H}^-$, $^{12}\text{C}_2^-$, $^{12}\text{C}^{14}\text{N}^-$, $^{31}\text{P}^-$, $^{34}\text{S}^-$ and $^{195}\text{Pt}^-$ secondary ions for platinum distribution measurements and $^1\text{H}^-$, $^2\text{H}^-$, $^{16}\text{O}^1\text{H}^-$, $^{16}\text{O}^2\text{H}^-$, $^{12}\text{C}_2^-$, $^{12}\text{C}^{13}\text{C}^-$ and $^{12}\text{C}^{14}\text{N}^-$ for ligand distribution measurements. Prior to data acquisition, analysis areas were pre-conditioned *in situ* by rastering of a high intensity, defocused Cs^+ ion beam in the following sequence of high and extreme low ion impact energies (HE / 16 keV and EXLIE / 50eV, respectively): HE at 100 pA beam current to a fluence of $5.0\text{E}14$ ions/cm²; EXLIE at 400 pA beam current to a fluence of $5.0\text{E}16$ ions/cm²; HE to a fluence of $2.5\text{E}14$ ions/cm². All data were acquired as multilayer image stacks obtained by sequential scanning of a finely focused Cs^+ primary ion beam over area of $42 \times 42 \mu\text{m}^2$ with 512×512 pixel image resolution. The physical resolution (probe size) was approx. 80 nm. The per-pixel dwell time of the primary ion beam was 10 ms.

NanoSIMS image processing and numerical data evaluation

NanoSIMS image data were evaluated by using the WinImage software package (version 2.0.8) provided by Cameca. Prior to stack accumulation, the individual images were drift corrected. Individual ROIs, representative for distinct cellular compartments, were defined manually. Secondary ion signal intensities were corrected for detector dead time on a per-pixel basis and quasi-simultaneous arrival (QSA) of C_2^- and CN^- secondary ions on a per-ROI basis. The QSA correction was performed according to the formalism suggested by previous work,⁸ applying sensitivity factors of 1.06, 1.05 and 1.0 for C_2^- , CN^- and other ions, respectively (experimentally determined on dried yeast cells – data not shown). $^2\text{H}/(^1\text{H} + ^2\text{H})$ and $^{13}\text{C}/(^{12}\text{C} + ^{13}\text{C})$ isotope fractions, given in atom percent (at. %) were calculated by

$$\frac{^2\text{H}}{^1\text{H} + ^2\text{H}} = \frac{^2\text{H}^-}{^1\text{H}^- + ^2\text{H}^-}$$

and

$$\frac{^{13}\text{C}}{^{12}\text{C} + ^{13}\text{C}} = \frac{^{12}\text{C}^{13}\text{C}^-}{2^{12}\text{C}_2^- + ^{12}\text{C}^{13}\text{C}^-}$$

where the symbols in the terms on the right-hand side refer to the signal intensities of each of the detected secondary ion species. The relative platinum content is displayed as the signal

intensity of $^{195}\text{Pt}^-$ normalized to the total C_2^- signal intensity, with the latter being utilized as reference signal. The calculation was performed via the following two formulas

$$\frac{^{195}\text{Pt}^-}{\text{C}_2^-} = \left(\frac{^{195}\text{Pt}^-}{^{12}\text{C}_2^-} \right)_{\text{Pt}} \times \left(\frac{^{12}\text{C}_2^-}{\text{C}_2^-} \right)_{2\text{H},^{13}\text{C}}$$

$$\frac{^{12}\text{C}_2^-}{\text{C}_2^-} = \frac{^{12}\text{C}_2^-}{^{12}\text{C}_2^- + ^{12}\text{C}^{13}\text{C}^- + ^{13}\text{C}_2^-} = \frac{^{12}\text{C}_2^-}{^{12}\text{C}^{13}\text{C}^- + ^{12}\text{C}_2^- (1 + R_{^{13}\text{C}/^{12}\text{C}}^2)}$$

where R refers to the isotopic ratio of ^{13}C over ^{12}C , obtained from the signal intensity ratios by

$$R_{^{13}\text{C}/^{12}\text{C}} = \frac{^{12}\text{C}^{13}\text{C}^-}{2^{12}\text{C}_2^-}$$

and the subscripts Pt and $^{2\text{H},^{13}\text{C}}$ designate the measurement run in which the respective signals were detected. Following the procedure applied in two previous publications,^{7, 9} the distribution of the DACH ligand is presented as the hydrogen content originating from the ligand relative to the total hydrogen content within the analyzed region. This quantity, referred to as $n_{\text{H,DACH}}/n_{\text{H,tot}}$ can be obtained by variable transformation of the $^2\text{H}/(^1\text{H} + ^2\text{H})$ isotope fractions (designated as “a”) of the DACH ligand and the isotope fractions measured in the sample as well as in an unlabeled control

$$\frac{n_{\text{H,DACH}}}{n_{\text{H,tot}}} = \frac{a_{2\text{H,tot}} - a_{2\text{H,ctrl}}}{a_{2\text{H,DACH}} - a_{2\text{H,ctrl}}}$$

By referencing the platinum signal ($^{195}\text{Pt}^-$) to the total hydrogen signal ($^1\text{H}^- + ^2\text{H}^-$) and plotting versus $n_{\text{H,DACH}}/n_{\text{H,tot}}$, relative stoichiometric changes in the drug composition through cellular uptake and compartmentalization can be revealed. It should be noted that this representation only makes sense if the isotopic label content measured in the sample is significantly higher than measured in the unlabeled control. As such, we constricted presentation of the ^{13}C measurement data to the $^{13}\text{C}/(^{12}\text{C} + ^{13}\text{C})$ isotope fractions.

ROI data were analyzed for normal distribution (Kolmogorov-Smirnov test, $p < 0.05$). Normally, distributed data were tested for significant differences in the arithmetic means by application of Welch's *t*-test, not normally distributed datasets were tested for significant differences in the medians by application of the Mann-Whitney *U*-test. Statistical calculations were conducted in the GraphPad Prism software (GraphPad Software Inc.), TEM/NanoSIMS overlay

images were generated utilizing the GIMP 2.10.6 software (GNU Image Manipulation Program).

Statistics

Results were analyzed and illustrated and statistical analyses performed (as indicated) with GraphPad Prism (GraphPad Software version 8, San Diego, CA).

2. Supplementary Figures

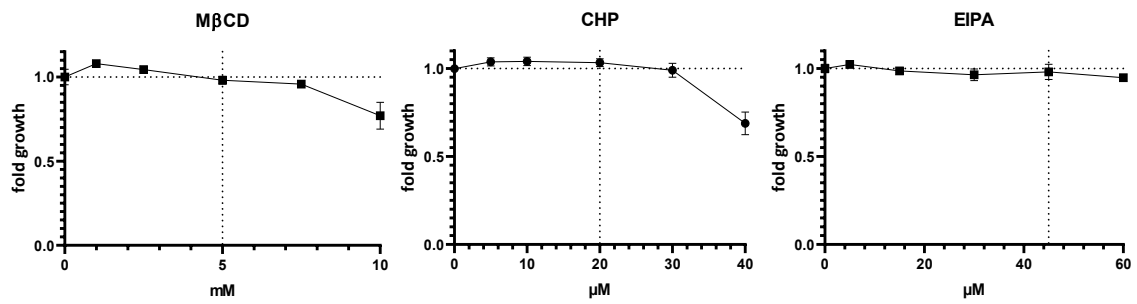


Figure S1. Impact of endocytosis inhibitors on cell viability. CT26 cells were treated with the endocytosis inhibitors methyl- β -cyclodextrin (M β CD), chlorpromazine (CHP) and 5-(N-ethyl-N-isopropyl)amiloride (EIPA) in rising concentrations for 5 h. Cell viability was determined by a MTT-based assay after 24 h. Values given are means \pm SD of one representative experiment performed in triplicates.

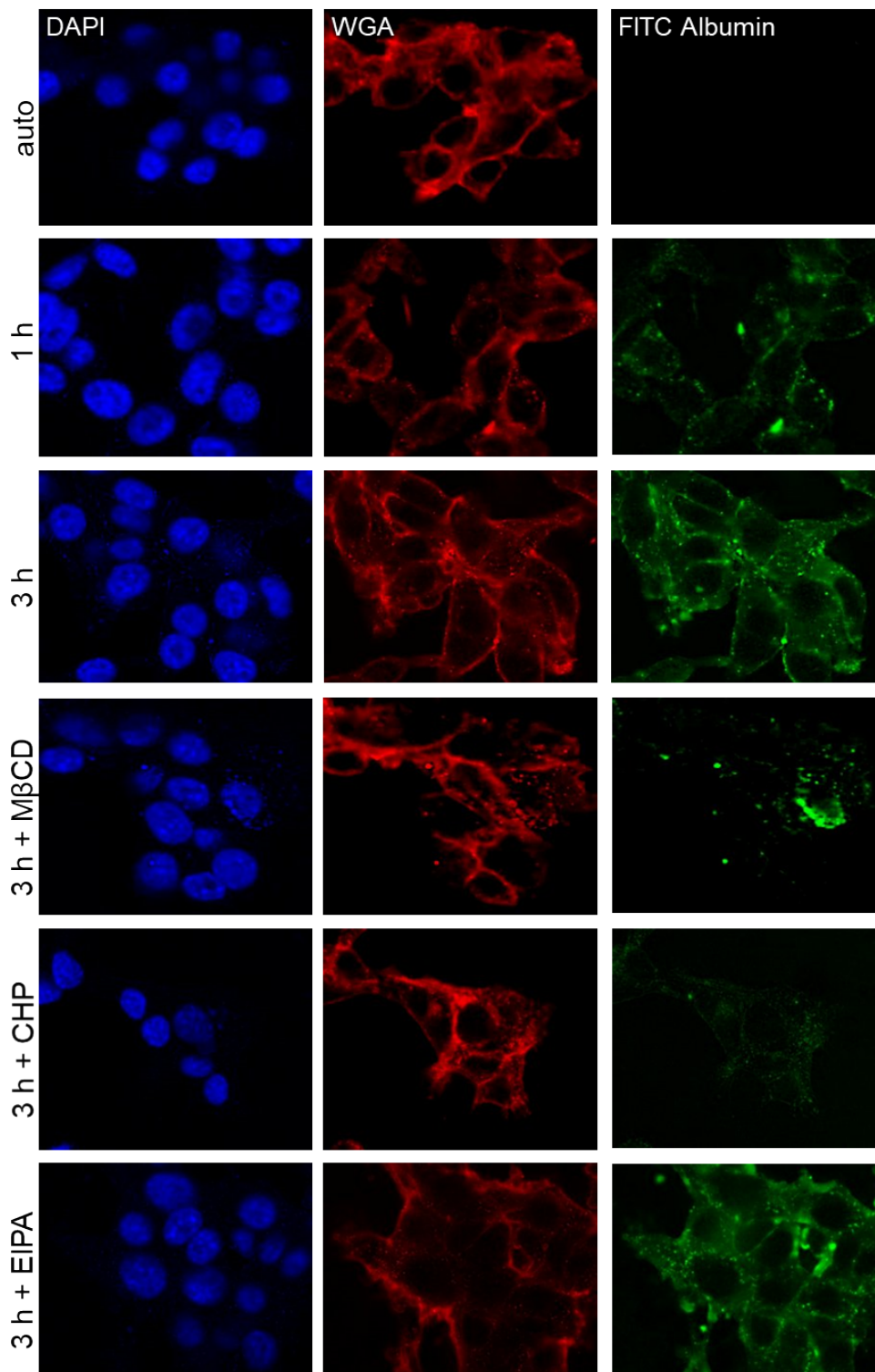


Figure S2. Uptake of FITC-labeled albumin (green) in CT26 cells and the impact of the three indicated endocytosis inhibitors was verified by confocal microscopy. Nuclei (blue) and membranes (red) were co-stained by DAPI and WGA, respectively.

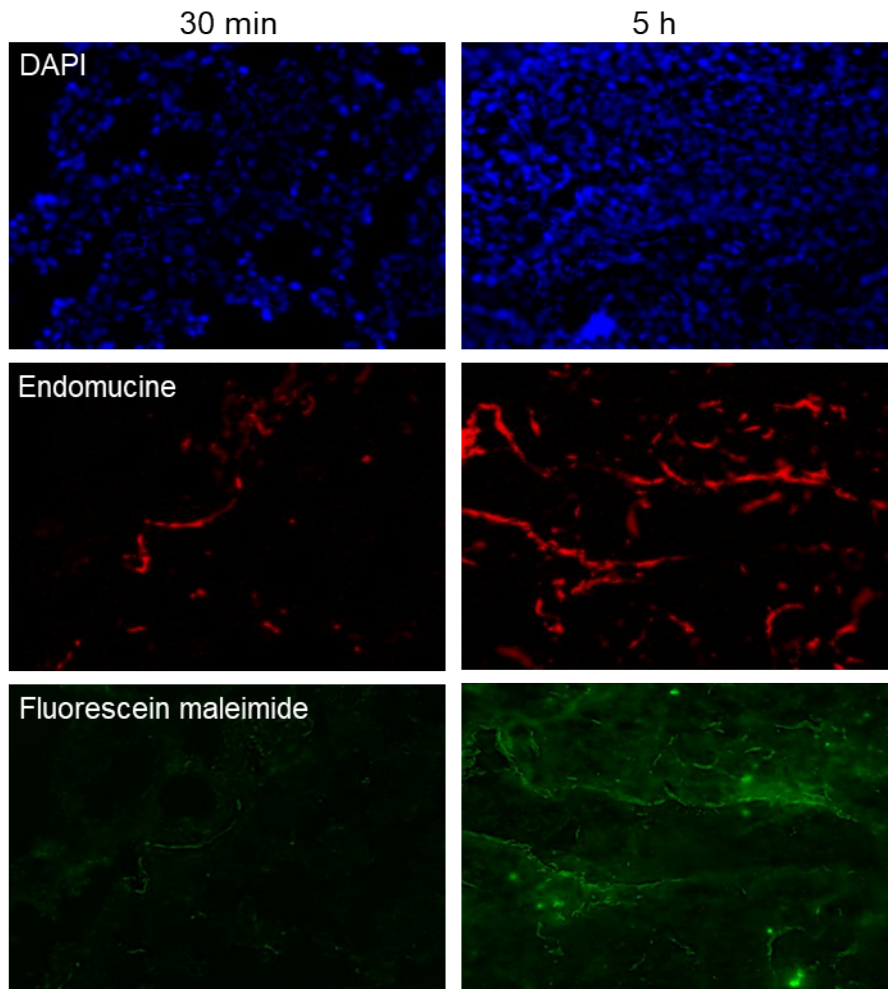


Figure S3. CT26-bearing male Balb/c mice were treated i.v. with 16.5 mg kg^{-1} fluorescein-labeled maleimide (green). After 30 min and 5 h the tumors were harvested followed by immunofluorescence staining of the nuclei (DAPI, blue) and the blood vessels (endomucine, red). Evaluation was done by fluorescence microscopy using a 40x objective.

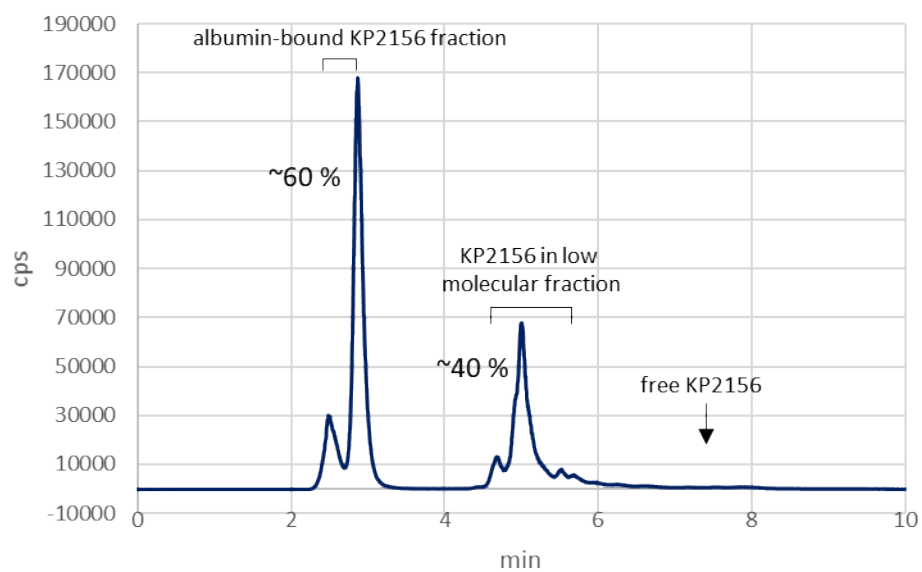


Figure S4. SEC-ICP-MS measurements of albumin binding after 2 h incubation of 100 μ M KP2156 in FCS and before dilution with cell culture medium.

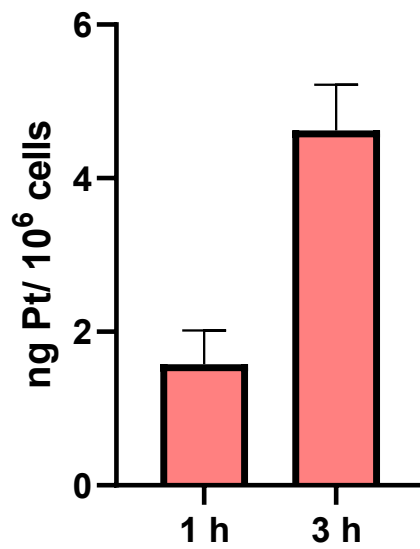


Figure S5. CT26 cells were treated for 1 h and 3 h with 10 μ M oxaliplatin. The cellular uptake of the drug was determined via ICP-MS measurements. Values are given as means \pm SD of three independent experiments.

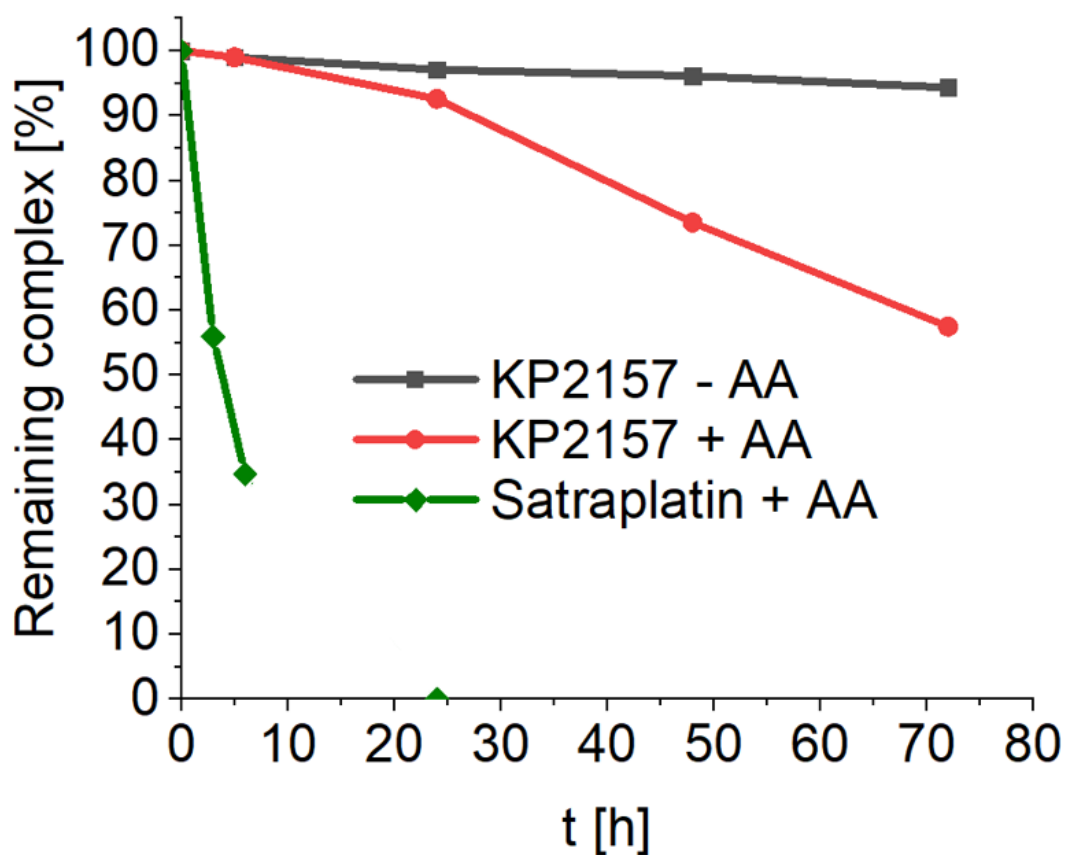


Figure S6. Reduction kinetics of KP2157 and satraplatin measured by NMR spectroscopy. 100 μM of KP2157 or satraplatin were incubated in deuterated phosphate buffer (100 mM, pD 7.4) at 37°C, with and without a 10-fold excess of ascorbic acid (AA). ^1H -NMR spectra were taken after 0, 5, 24, 48 and 72 h.

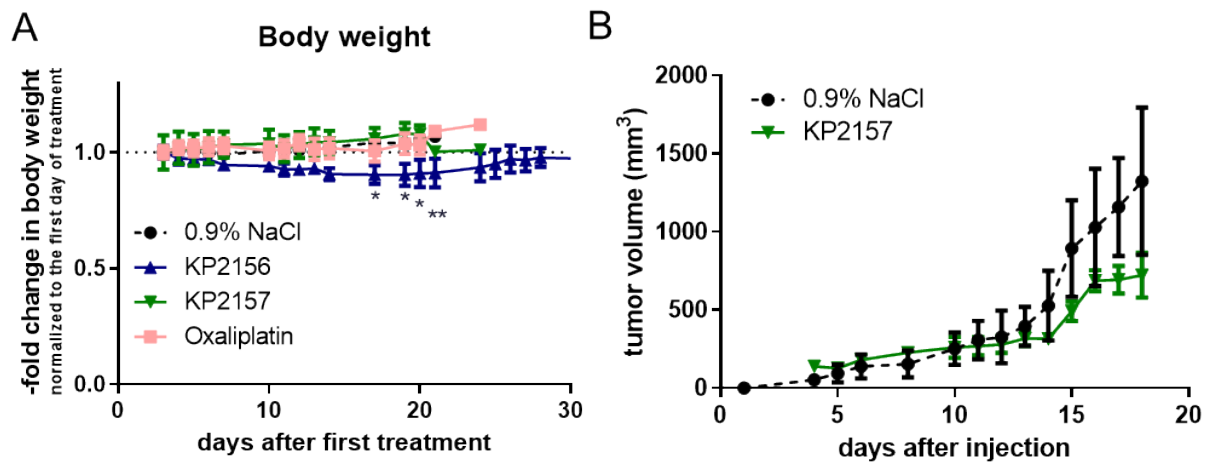


Figure S7. CT26-bearing Balb/c mice (male) were treated with the indicated drugs equimolar to 9 mg kg⁻¹ oxaliplatin i.v. twice a week for two weeks. Data are means ± SEM. Statistical significance was tested by two-way ANOVA (*p < 0.05, ** p < 0.01). (A) shows the change in body weight during therapy. (B) shows the data of the tumor volume of KP2157 or 0.9% NaCl treated mice (n=4). Data are means ± SEM.

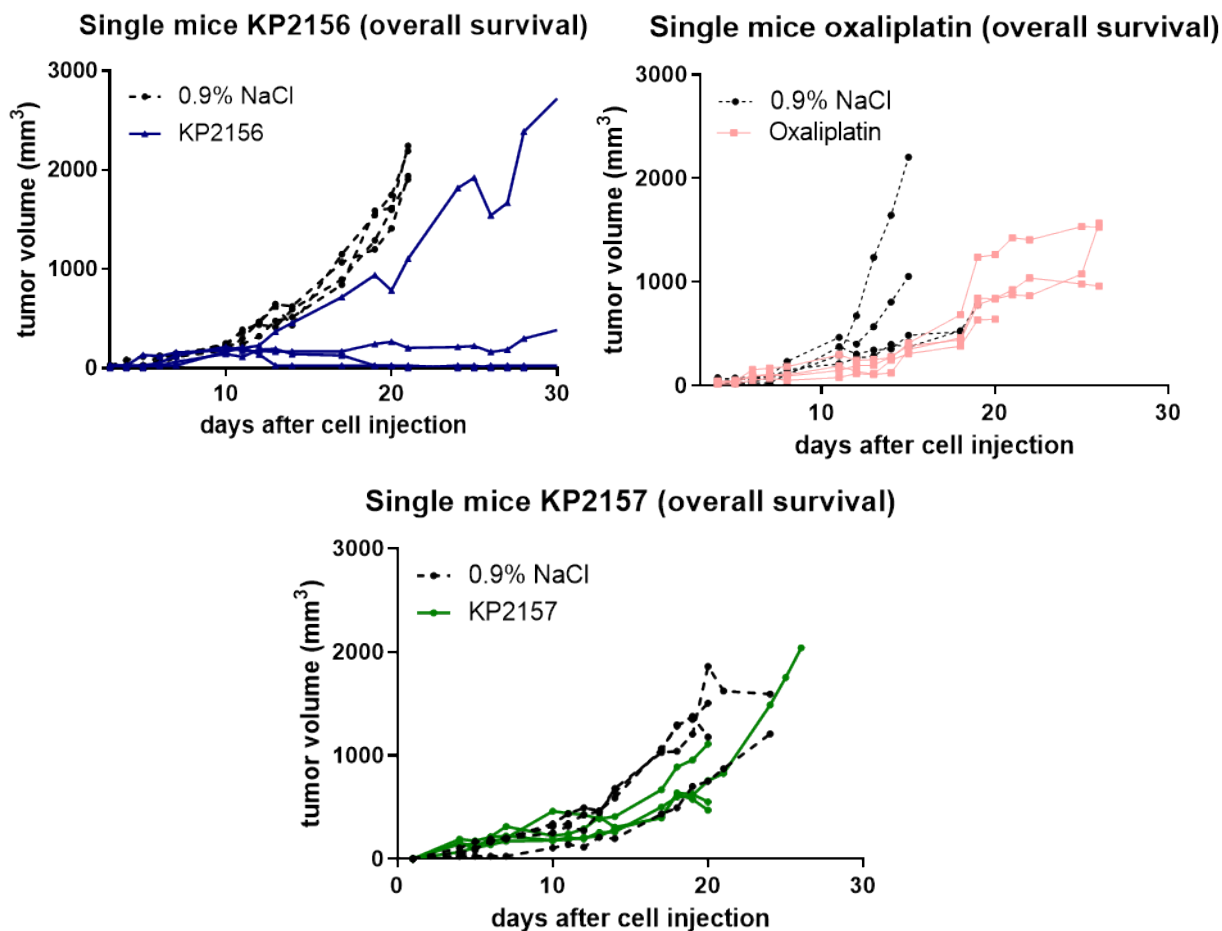


Figure S8. Tumor volume of the individual CT26-bearing mice after i.v. treatment of the indicated drugs (equimolar to 9 mg kg⁻¹ oxaliplatin, two times a week for two weeks). Endpoint of the experiments was overall survival.

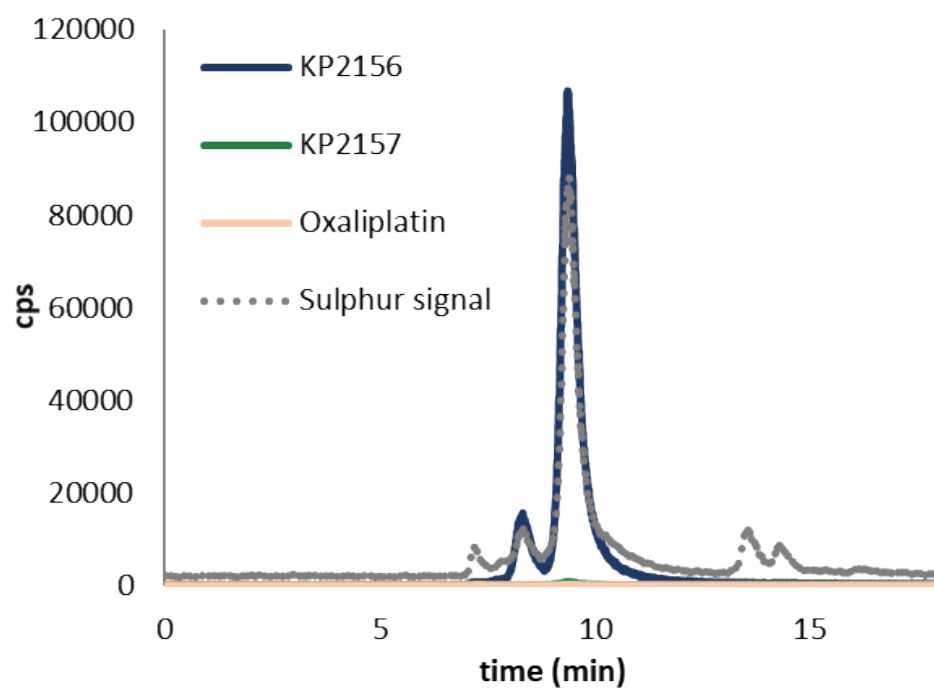


Figure S9. Exemplary chromatograms of SEC-ICP-MS analysis of blood serum of mice treated once i.v. with KP2156, KP2157 or oxaliplatin (equimolar to 9 mg kg⁻¹) for 30 min. KP2157, oxaliplatin and non-albumin bound KP2156 are already (nearly) completely excreted from the serum at this time point.

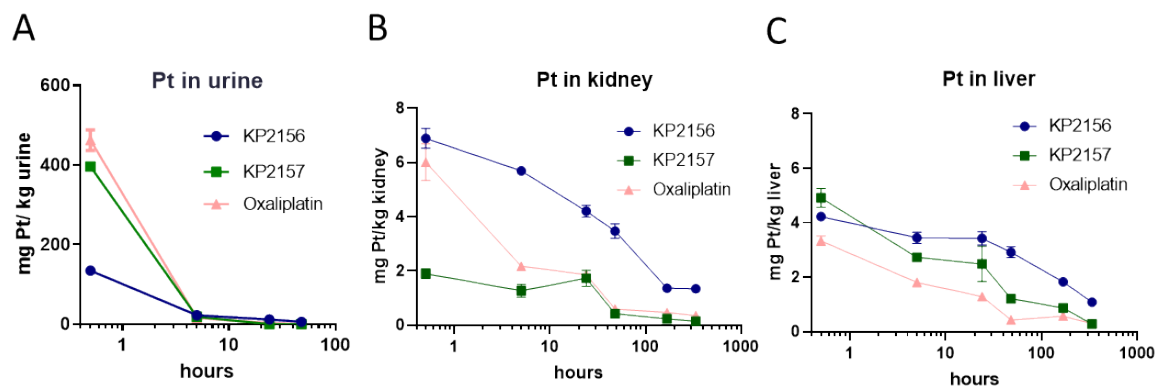


Figure S10. (A) Balb/c mice (male) were treated with a single dose of KP2156, KP2157 and oxaliplatin (all equimolar to 9 mg kg⁻¹ oxaliplatin). After different time points (5 h, 24 h, 48 h, 168 h and 336 h) animals were dissected and urine (A), kidney (B) and liver (C) were collected. Platinum levels were determined via ICP-MS measurements. Values are means ± SEM.

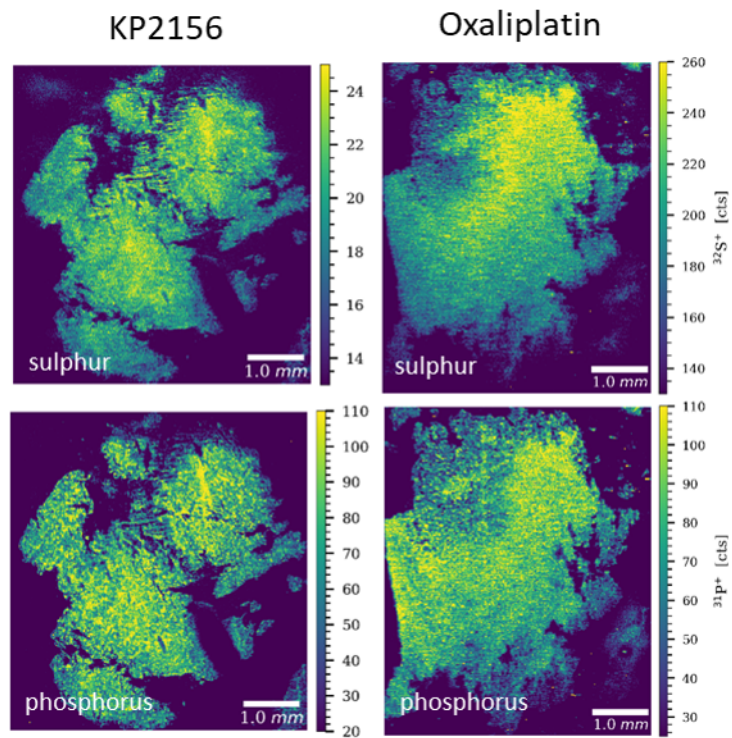


Figure S11. Intratumoral distribution of sulphur and phosphorus in KP2156- (equimolar to 9 mg kg^{-1} oxaliplatin, i.v.) and oxaliplatin-treated (9 mg kg^{-1} , i.v.) CT26 tumors after 5 h. Tissues were analyzed by LA-ICP-MS.

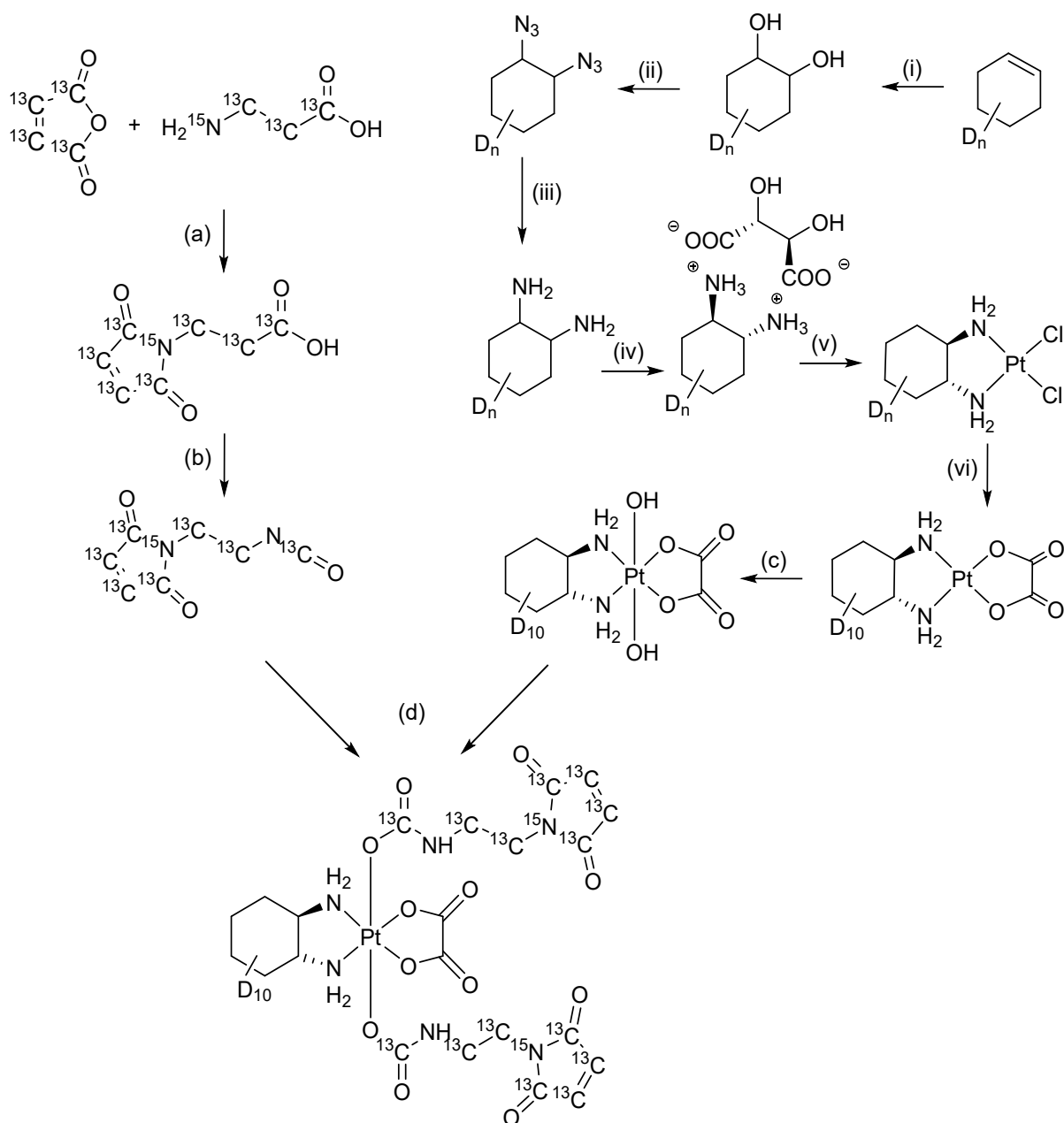


Figure S12. Synthesis of the isotopically-labeled complex KP2603. Reaction steps of oxaliplatin synthesis: (i) $\text{H}_2\text{O}_2/\text{HCOOH}$, (ii) MsCl/Py , NaN_3 , (iii) Pd/CaCO_3 , H_2 (3 bar), (iv) L-tartaric acid, (v) $\text{K}_2\text{PtCl}_4/\text{NaOH}$ (0.25 M) and (vi) AgNO_3 , potassium oxalate. Reaction steps of KP2603 synthesis: (a) acetic acid, 170°C , HPLC purification (b) acetone, ethyl chloroformate, NaN_3 , Et_3N (c) H_2O , H_2O_2 , (d) DMF, HPLC purification.

Figure S13. HPLC run at 225 nm showing >98% purity of KP2603

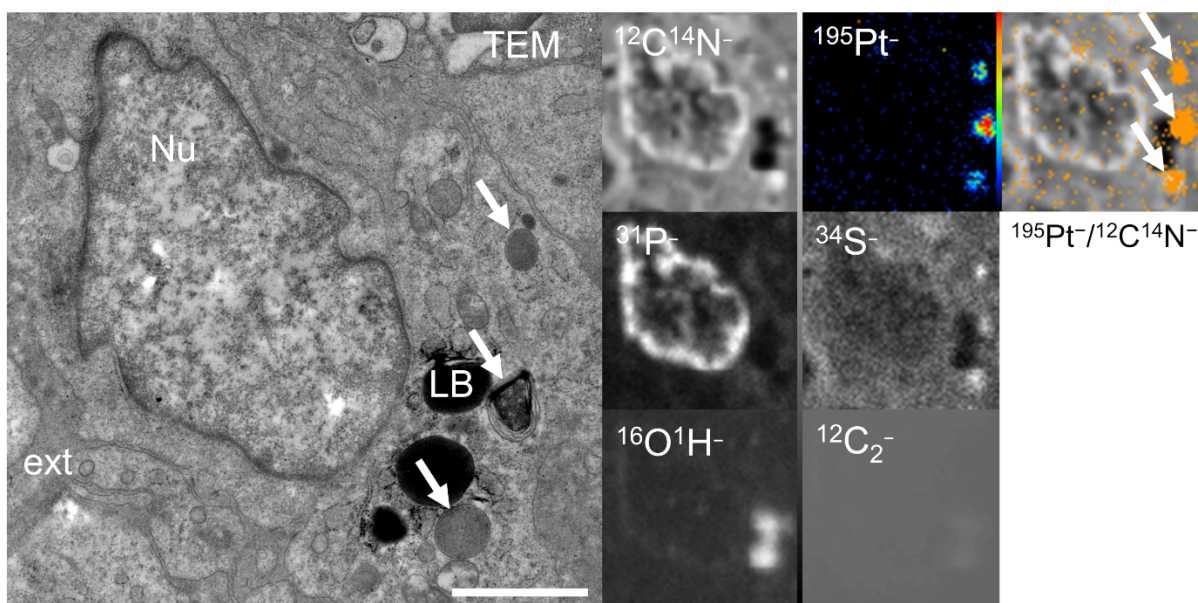


Figure S14. Platinum distribution in cancer cells from a CT26 tumor-bearing mouse upon treatment with KP2603. NanoSIMS $^{12}\text{C}^{14}\text{N}^-$, $^{195}\text{Pt}^-$, $^{31}\text{P}^-$, $^{34}\text{S}^-$, $^{16}\text{O}^1\text{H}^-$ and $^{12}\text{C}_2^-$ secondary ion maps show the subcellular localization of the signal intensities in an ultra-thin section of malignant tissue. Intensities are displayed on a false color scale ranging from low intensities (black) to high intensities (red/white). TEM micrograph displaying the ultrastructure of the corresponding area from a same resin section. White arrows indicate platinum accumulating structures inside the cell cytoplasm; in the overlay image, the $^{12}\text{C}^{14}\text{N}^-$ signal intensity is displayed on a gray scale, the orange dots refer to areas with $^{195}\text{Pt}^-$ signal intensities of ≥ 1 count/pixel. Abbreviations: ext – extracellular matrix; LB – lipid bodies; Nu – nucleus; Scale bar = 1 μm .

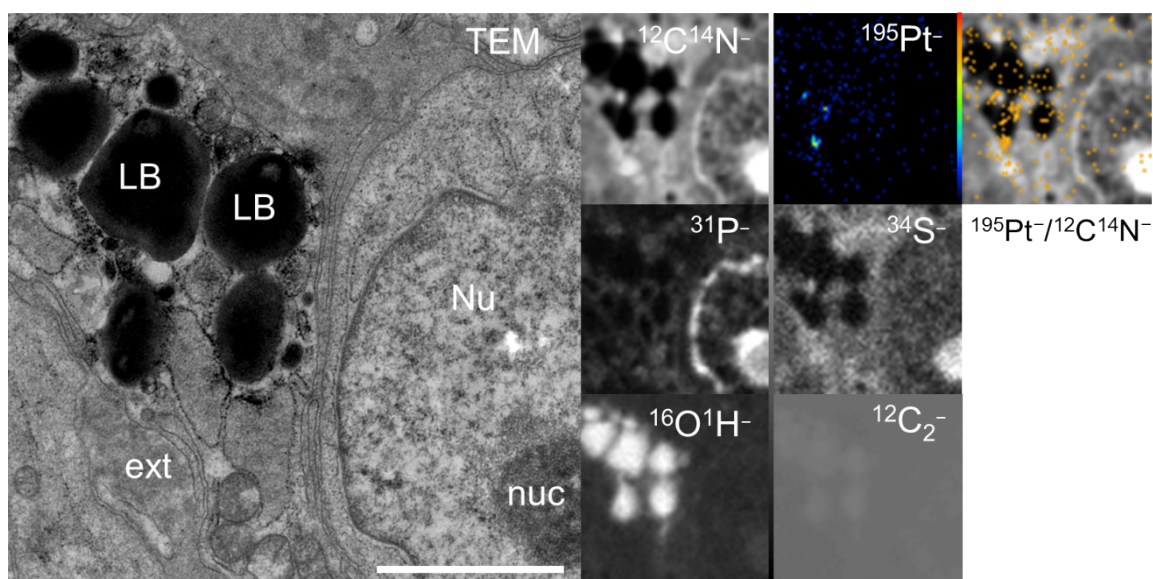


Figure S15. Platinum distribution in cancer cells from a CT26 tumor-bearing mouse upon treatment with KP2603. NanoSIMS $^{12}\text{C}^{14}\text{N}^-$, $^{195}\text{Pt}^-$, $^{31}\text{P}^-$, $^{34}\text{S}^-$, $^{16}\text{O}^1\text{H}^-$ and $^{12}\text{C}_2^-$ secondary ion maps show the subcellular localization of the signal intensities in an ultra-thin section of malignant tissue. Intensities are displayed on a false color scale ranging from low intensities (black) to high intensities (red/white); in the overlay image, the $^{12}\text{C}^{14}\text{N}^-$ signal intensity is displayed on a gray scale, the orange dots refer to areas with $^{195}\text{Pt}^-$ signal intensities of ≥ 1 count/pixel. TEM micrograph displaying the ultrastructure of the corresponding area from a same resin section. Note the enhanced $^{16}\text{O}^1\text{H}^-$ signal intensity detected within lipid bodies, which indicates an enhanced oxygen and hydrogen content in this cellular compartment (see Fig. S17). Abbreviations: ext – extracellular matrix; LB – lipid bodies; Nu – nucleus; nuc – nucleolus; Scale bar = 1 μm .

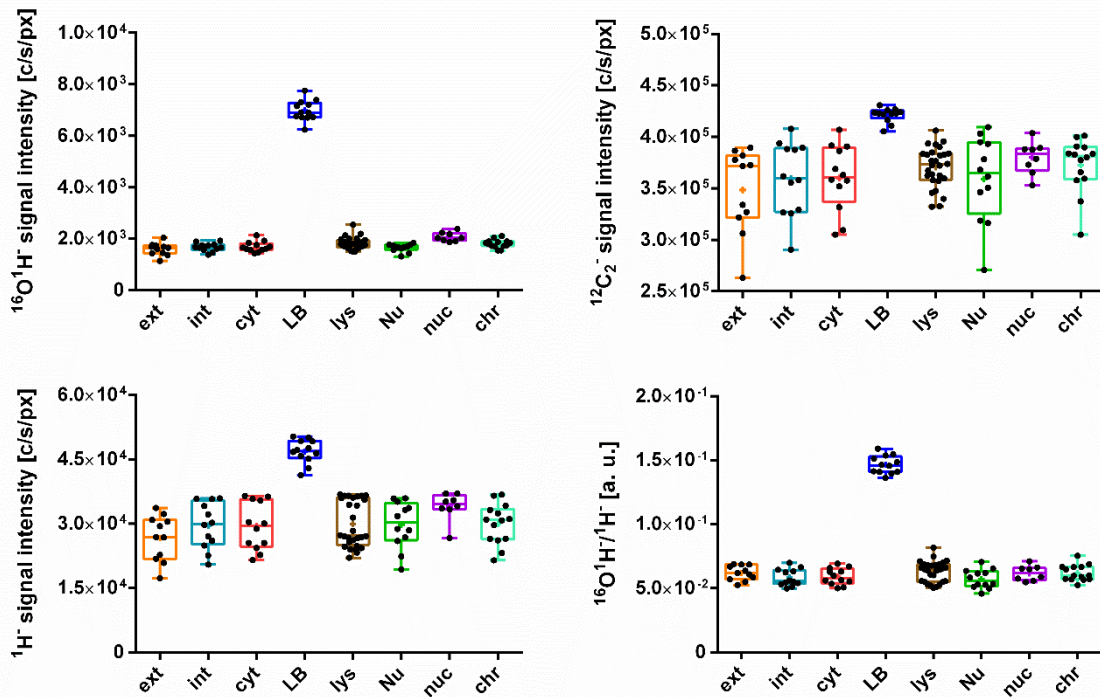


Figure S16. Relative enhancement of the carbon, oxygen and hydrogen contents within lipid bodies (LB) in comparison to other compartments as revealed by NanoSIMS elemental mapping. The relative oxygen content is referred to by the $^1\text{H}^-$ normalized $^{16}\text{OH}^-$ signal intensity since the limited number of detectors prevented simultaneous detection of $^{16}\text{O}^-$ secondary ions. Note that the analyzed samples were smooth and showed homogeneous erosion, which means that sputtering- and/or topography related effects on the signal intensities can be excluded. Abbreviations: ext – extracellular matrix, int – intracellular compartment (whole cells); cyt – cytoplasm; LB – lipid bodies; lys – lysosomes/platinum hotspots; Nu – nucleus; nuc – nucleolus; chr – chromatin; c/s/px – counts/(second*pixel).

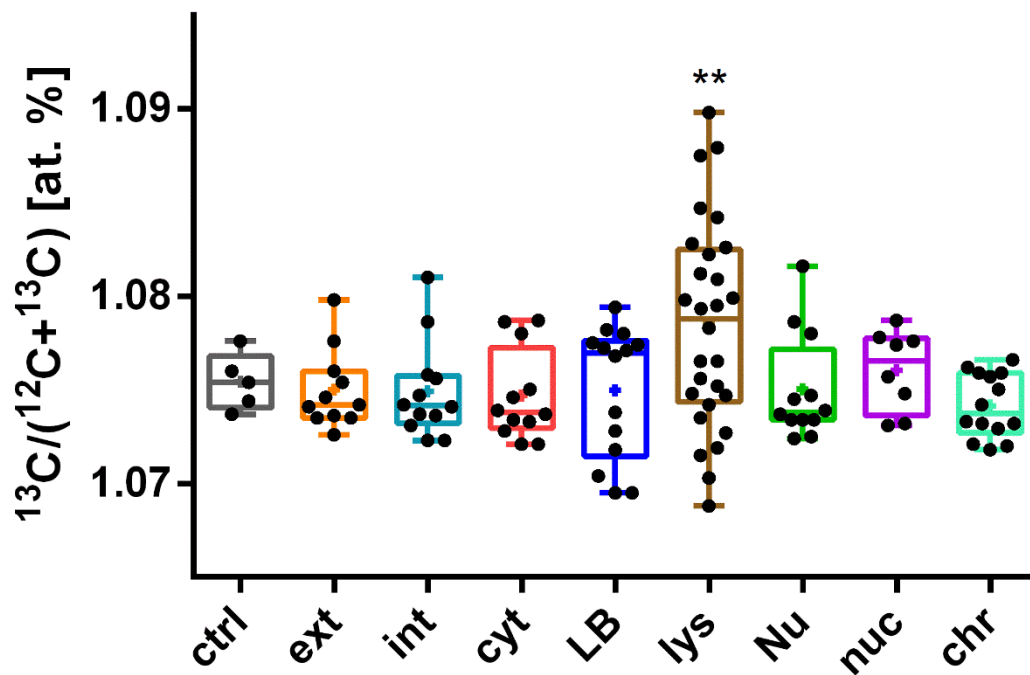


Figure S17. Subcellular distribution of the ^{13}C isotope label contents in KP2603 treated CT26 cells relative to an untreated control as inferred from NanoSIMS isotope selective mapping. Data points refer to individual ROI values. The box-and-whisker plots display the extreme values (min/max), median and lower/upper quartiles. Statistical analysis: Kolmogorov-Smirnov normality test followed by two-sided Student's t-test with Welch's correction or Mann-Whitney U-test (* $p < 0.05$, ** $p < 0.01$). Abbreviations and number of ROIs per category: ctrl – negative control (average values of tumor cells from an untreated mouse, $n = 5$), ext – extracellular matrix ($n = 11$), int – intracellular compartment (whole cells, $n = 12$); cyt – cytoplasm ($n = 12$); LB – lipid bodies ($n = 14$); lys – lysosomes/platinum hotspots ($n = 28$); Nu – nucleus ($n = 12$); nuc – nucleolus ($n = 8$); chr – chromatin ($n = 14$).

3. Supplementary Tables

Table S1. Pharmacokinetic parameters after KP2156, KP2157 or oxaliplatin treatment (i.v.).

	KP2156	KP2157	Oxaliplatin
D^{a)} [mg kg⁻¹]	18	18	9
Cl^{b)} [h]	0.012	0.316	0.141
t_{1/2}^{c)} [h]	55.72	25.67	32.48
AUC^{d)} [mg kg⁻¹*h⁻¹]	KP2156	KP2157	Oxaliplatin
Serum	1540	57	64
Tumor	833	42	77
Kidney	731	133	218
Liver	688	333	195
AUC Ratio	KP2156:KP2157	KP2156:Oxaliplatin	KP2157:Oxaliplatin
Serum	27	24.1	0.9
Tumor	19.8	10.9	0.5
Kidney	5.5	3.4	0.6
Liver	2.1	3.5	1.7
Relative Organ Enrichment	KP2156	KP2157	Oxaliplatin
Tumor/serum	0.5	0.7	1.2
Tumor/kidney	1.1	0.3	0.4
Tumor/liver	1.2	0.1	0.4

a) dose; b) total clearance; c) elimination half-life; d) area under the curve;

4. References

1. V. Pichler, J. Mayr, P. Heffeter, O. Domotor, E. A. Enyedy, G. Hermann, D. Groza, G. Kollensperger, M. Galanski, W. Berger, B. K. Keppler and C. R. Kowol, *Chem Commun (Camb)*, 2013, **49**, 2249-2251.
2. A. E. Egger, C. Rappel, M. A. Jakupec, C. G. Hartinger, P. Heffeter and B. K. Keppler, *J Anal At Spectrom*, 2009, **24**, 51-61.
3. C. Karnthaler-Benbakka, D. Groza, K. Kryeziu, V. Pichler, A. Roller, W. Berger, P. Heffeter and C. R. Kowol, *Angewandte Chemie (International ed. in English)*, 2014, **53**, 12930-12935.
4. M. A. Hoda, A. Mohamed, B. Ghanim, M. Filipits, B. Hegedus, M. Tamura, J. Berta, B. Kubista, B. Dome, M. Grusch, U. Setinek, M. Micksche, W. Klepetko and W. Berger, *Journal of thoracic oncology : official publication of the International Association for the Study of Lung Cancer*, 2011, **6**, 852-863.
5. S. Theiner, H. P. Varbanov, M. Galanski, A. E. Egger, W. Berger, P. Heffeter and B. K. Keppler, *Journal of biological inorganic chemistry : JBIC : a publication of the Society of Biological Inorganic Chemistry*, 2015, **20**, 89-99.
6. L. Habala, M. Galanski, A. Yasemi, A. A. Nazarov, N. G. von Keyserlingk and B. K. Keppler, *European journal of medicinal chemistry*, 2005, **40**, 1149-1155.
7. A. A. Legin, S. Theiner, A. Schintlmeister, S. Reipert, P. Heffeter, M. A. Jakupec, J. Mayr, H. P. Varbanov, C. R. Kowol, M. Galanski, W. Berger, M. Wagner and B. K. Keppler, *Chemical science*, 2016, **7**, 3052-3061.
8. G. Slodzian, F. Hillion, F. J. Stadermann and E. Zinner, *Appl Surf Sci*, 2004, **231-232**, 874-877.
9. A. A. Legin, A. Schintlmeister, N. S. Sommerfeld, M. Eckhard, S. Theiner, S. Reipert, D. Strohofer, M. A. Jakupec, M. Galanski, M. Wagner and B. K. Keppler, *Nanoscale Advances*, 2021, **3**, 249-262.